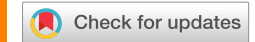
RESEARCH ARTICLE | OCTOBER 28 2025

# Growth and probing the band-to-impurity transitions in oxygen-doped h-BN $\ensuremath{ igoldsymbol{arphi}}$

Z. Alemoush [0]; M. Almohammad [0]; J. Li [0]; J. Y. Lin [0]; H. X. Jiang [ 0]



Appl. Phys. Lett. 127, 172105 (2025) https://doi.org/10.1063/5.0284827

A CHORUS





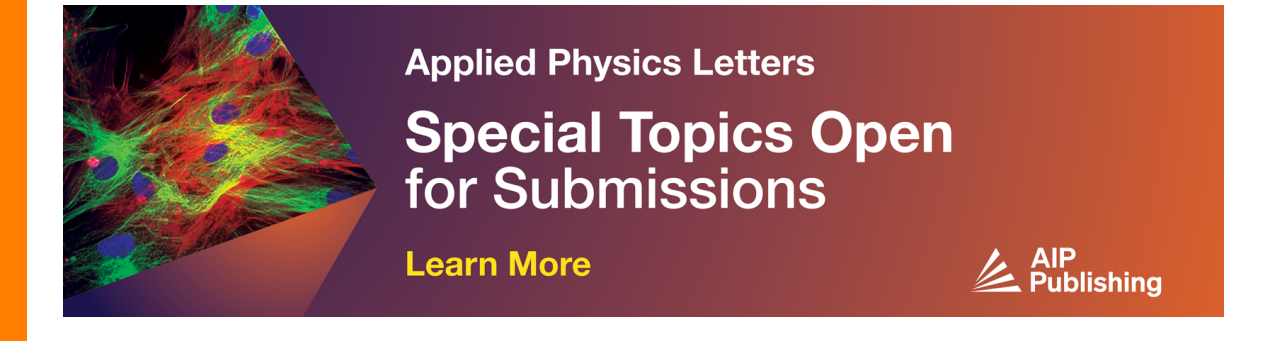
### Articles You May Be Interested In

Two-scale structure of the current layer controlled by meandering motion during steady-state collisionless driven reconnection

Phys. Plasmas (July 2004)

Single particle motion near an X point and separatrix

Phys. Plasmas (June 2004)





## Growth and probing the band-to-impurity transitions in oxygen-doped h-BN

Cite as: Appl. Phys. Lett. 127, 172105 (2025); doi: 10.1063/5.0284827 Submitted: 10 June 2025 · Accepted: 9 October 2025 · Published Online: 28 October 2025







Z. Alemoush, 🝺 M. Almohammad, 向 J. Li, 🍺 J. Y. Lin, 向 and H. X. Jiang<sup>a)</sup> 🝺

#### **AFFILIATIONS**

Department of Electrical and Computer Engineering, Texas Tech University, Lubbock, Texas 79409, USA

<sup>a)</sup>Author to whom correspondence should be addressed: hx.jiang@ttu.edu

#### **ABSTRACT**

Intentionally oxygen-doped hexagonal boron nitride (h-BN) thick epilayers have been produced using hydride vapor phase epitaxy (HVPE). Oxygen doping significantly enhanced the crystalline quality of h-BN, likely due to the reduced nitrogen vacancies by substitutional oxygen donors. By eliminating carbon impurity emission lines through HVPE growth, the origin of the commonly observed, yet poorly understood, emission lines in the 5.3-5.5 eV spectral region in h-BN can be definitively attributed to the recombination between electrons bound to substitutional oxygen donors on nitrogen sites (O<sub>N</sub>) and free holes in the valence band, along with phonon replicas involving K-point phonons via a strong hole-phonon interaction, a result of its indirect energy bandgap nature. Unlike the generally "dark" band-to-band and excitonic transitions in perfect h-BN, the zero-phonon line of the oxygen donor-related band-to-impurity transition prominently contributes to the emission intensity due to the deep-level nature of oxygen donors. This study resolves the long-standing question of the physical origin of the 5.3 eV emission line in h-BN, providing a more comprehensive understanding of common impurities/defects in h-BN, which is vital for monitoring and continuously improving the material quality and purity of h-BN, paving the way for future applications of this emerging ultrawide bandgap (UWBG) semiconductor.

Published under an exclusive license by AIP Publishing. https://doi.org/10.1063/5.0284827

Hexagonal boron nitride (h-BN) is a material of significant interest, owing to its intriguing fundamental properties and broad potential applications. These include deep-ultraviolet (DUV) optoelectronic devices, <sup>1-4</sup> direct conversion solid-state neutron detectors, <sup>5-11</sup> single photon emitters, <sup>12</sup> and two-dimensional heterojunction devices. <sup>13</sup> While substantial progress has been made in h-BN material growth and understanding its band structure, optical, thermal, and electrical transport properties, 16-28 the fundamental properties of defects and impurities remain less understood compared to traditional III-nitride semiconductors. Theoretical predictions suggest that all impurities in h-BN are quite deep, <sup>29,30</sup> which significantly hinders doping prospects. Among known impurities and defects, oxygen was predicted to occupy the nitrogen site (O<sub>N</sub>), forming a relatively shallow donor, with a calculated energy level of approximately 0.6 eV.<sup>29</sup> Experimental evidence widely indicates that oxygen is readily incorporated into h-BN through various pathways, such as diffusion from sapphire substrates, surface oxidation, and contamination from reactor components. This pervasive incorporation is attributed to h-BN's layered crystalline structure and the large bond energy of the B-O bond. While the influence of oxygen impurities on the optical and transport properties of GaN and AlN has been thoroughly investigated, 31-33 the role of oxygen

impurities in h-BN is considerably less explored. Investigating bandto-impurity transitions is a powerful method for characterizing impurity properties, offering insights into the band structure, impurity energy levels, and material purity. However, the ultrawide and indirect nature of h-BN's bandgap necessitates a reevaluation and modification of the conventional understanding of impurity transitions.

In direct bandgap semiconductors like GaN and AlN, both the conduction band minimum (CBM) and valence band maximum (VBM) are located at the  $\Gamma$ -point, the center of the Brillouin zone (BZ). Energies at other high-symmetry points within the first BZ, such as the L- and X-points, are significantly higher than those at the  $\Gamma$ -point in these materials. Consequently, all fundamental optical transitions in GaN and AlN occur at the  $\Gamma$ -point, and their electronic properties are predominantly governed by the band parameters at this point.<sup>34</sup> In stark contrast, h-BN exhibits an indirect bandgap where the CBM and VBM are situated at different high-symmetry points: the CBM at the M-point and the VBM at the K-point. 17-23 Upon photoexcitation above the bandgap, electrons relax to the CBM at the M-point, while holes relax to the VBM at the K-point. In this regard, band-toimpurity transitions in h-BN resemble free exciton transitions, which are well-established to require phonon assistance for momentum

conservation in perfect h-BN crystals. <sup>17-23</sup> Therefore, band-to-impurity transitions in h-BN are also expected to involve phonons for momentum conservation. However, a critical distinction for band-to-impurity transitions in h-BN is that the wavefunctions of electrons or holes bound to deep donors or acceptors can extend across multiple high-symmetry points in the BZ, encompassing both M- and K-points. This phenomenon arises because impurity energy levels in h-BN are deep, and the energy difference between the M- and K-points in the conduction band is relatively small. <sup>17-23,28</sup>

The most frequently observed and studied impurity emission line in h-BN is centered around 4.1 eV, which is typically attributed to the presence of carbon impurities. This 4.1 eV line often overwhelmingly dominates the photoluminescence (PL) emission spectra of h-BN grown by metalorganic chemical vapor deposition (MOCVD), particularly when using triethylborane (TEB) or trimethylborane (TMB) as boron precursors, which inherently contain carbon. Other emission lines appearing in the 5.3–5.5 eV spectral region are also frequently reported in h-BN thin films. These become more pronounced in MOCVD materials produced under high NH3 flow rates, conditions that significantly suppress the 4.1 eV emission line. Several mechanisms have been proposed to explain the origin of these 5.3–5.5 eV lines, including multi-phonon-assisted excitonic transitions, bund excitons, and stacking disorder.

In this work, we produced h-BN with intentional oxygen doping using hydride vapor phase epitaxy (HVPE) and performed PL emission spectroscopy studies. By utilizing BCl<sub>3</sub> gas as a boron precursor in HVPE growth, we avoided the incorporation of carbon impurities, thereby eliminating the 4.1 eV optical transition line. This simplification

significantly aided the understanding of oxygen-related emission lines in h-BN. Our results unambiguously conclude that all emission lines observed in the 5.3–5.5 eV spectral region share the same physical origin: a band-to-impurity transition involving the recombination between electrons bound to  $\rm O_N$  donors and free holes, along with its phonon replicas. We also provide a general discussion on the major differences in band-to-impurity transition characteristics between indirect bandgap h-BN and other direct bandgap III-nitride semiconductors.

Undoped and oxygen-doped h-BN (h-BN:O) epilayers with a thickness of  ${\sim}50\,\mu m$  were grown on c-plane sapphire (Al<sub>2</sub>O<sub>3</sub>) substrates by HVPE using BCl<sub>3</sub> and ammonia (NH<sub>3</sub>) as precursors for B and N, respectively. Pure oxygen gas was used as an oxygen dopant source and carried into the reactor by N<sub>2</sub> gas using a flow rate of 5 sccm. No hydrogen was introduced at any stage of growth to eliminate the potential effects associated with hydrogen incorporation. A low-temperature undoped BN buffer layer of 20 nm in thickness was deposited on sapphire at 1200 °C prior to the growth of oxygen-doped h-BN epilayers to minimize the impact of lattice mismatch between h-BN and Al<sub>2</sub>O<sub>3</sub>. The h-BN epilayers were grown at 1500 °C using a growth rate of  ${\sim}20\,\mu m/h$ .

The inset of Fig. 1(a) plots the oxygen concentration as a function of the sample depth, probed by secondary-ion mass spectrometry (SIMS). Since the growth and doping conditions remained the same during the growth process, the doping concentration of about  $7 \times 10^{19}$  cm<sup>-3</sup> atoms/cm<sup>3</sup> at 1  $\mu$ m depth and beyond should represent the oxygen doping concentration in the sample's interior, by neglecting the artifacts induced by the surface oxidation effect. Figure 1 presents structural characterization results among undoped h-BN and oxygendoped h-BN (h-BN:O) wafers: (a) x-ray diffraction (XRD) patterns in

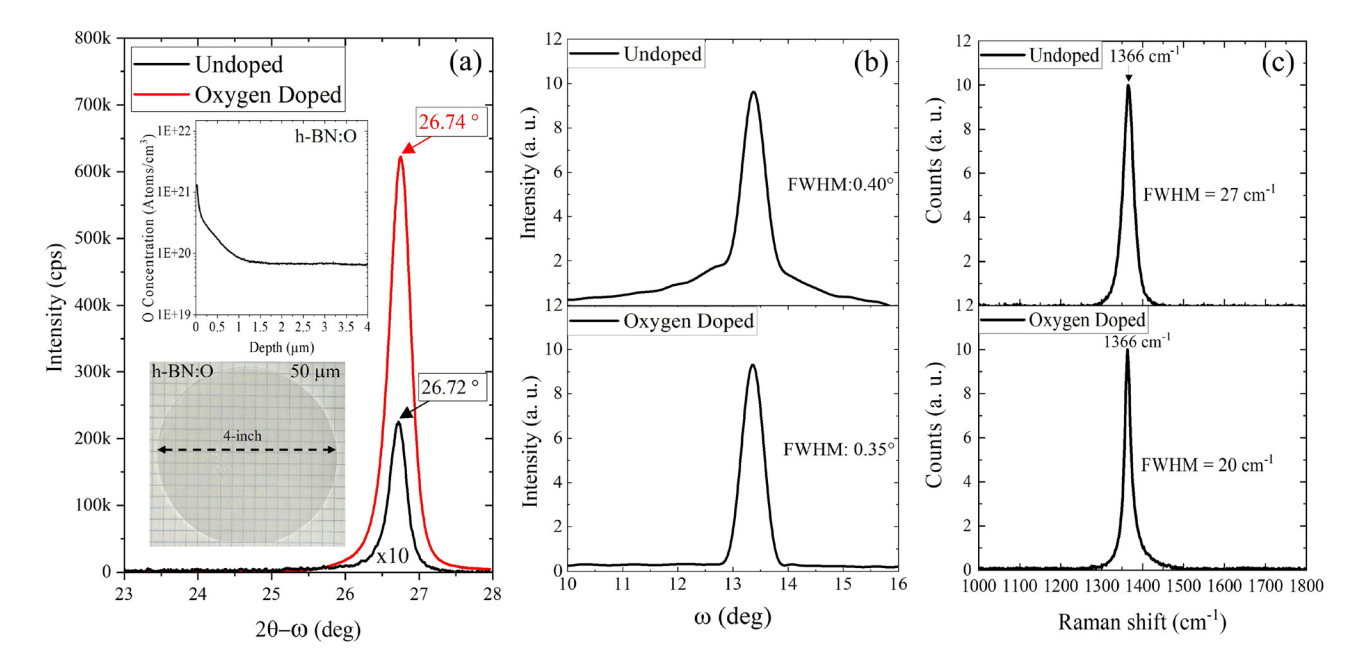


FIG. 1. (a) Comparison of x-ray diffraction (XRD) patterns in  $2\theta-\omega$  scans among undoped h-BN and oxygen-doped h-BN (h-BN:O) wafers of 50 μm in thickness. The inset shows an optical micrograph of a 4"-diameter freestanding h-BN:O wafer and oxygen doping profile in the wafer probed by secondary mass spectrometry (SIMS). (b) Comparison of XRD rocking curves ( $\omega$ — scans) of (002) diffraction peak among undoped h-BN and oxygen-doped h-BN (h-BN:O) wafers. (c) Comparison of Raman spectra among undoped h-BN and oxygen-doped h-BN (h-BN:O) wafers.

 $2\theta - \omega$  scans, (b) XRD rocking curves ( $\omega$  – scans) of (002) diffraction peak, and (c) Raman spectra. The results clearly demonstrate that oxygen doping significantly enhances the overall crystalline quality of h-BN. This improvement is evidenced by several key observations: (1) a shift of the h-BN (002) peak (representing diffraction from planes stacked along the c-direction) from 26.72° to the ideal h-BN value of 26.74° in h-BN:O wafer; (2) a remarkable increase in the h-BN (002) peak intensity by a factor of more than 30 in h-BN:O wafer; (3) the full width at half maximum (FWHM) of XRD rocking curve is reduced in h-BN:O wafer compared to undoped wafer (from 0.4° to 0.35°); and (4) the FWHM of the  $E_{2g}$  vibration mode (in-plane stretch of B and N atoms) at  $\Delta \sigma = 1366 \, \mathrm{cm}^{-1}$  observed in the Raman spectrum of h-BN:O wafer is also significantly reduced compared to undoped sample (from 27 and 20 cm<sup>-1</sup>). We believe that the enhanced structural ordering observed in oxygen-doped h-BN is because oxygen impurities act as substitutional donors on nitrogen sites (O<sub>N</sub>) in h-BN.<sup>29</sup> This substitution reduces the number of nitrogen vacancies, leading to a more ordered structure.

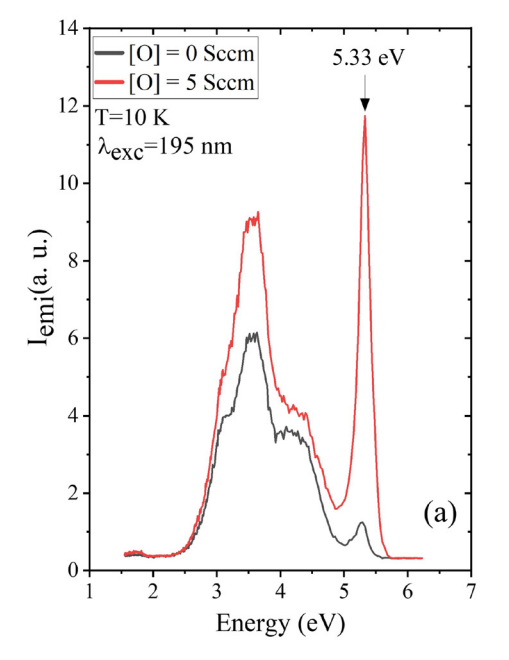
Figure 2(a) presents a comparative analysis of the low-temperature (10 K) PL emission spectra from undoped (black curve) and oxygen-doped (red curve) h-BN. In the undoped sample, the emission line near 5.33 eV is very weak, with its presence most likely attributable to surface oxidation of the h-BN.<sup>46</sup> In sharp contrast, this 5.33 eV line becomes overwhelmingly dominant in the h-BN:O sample, strongly supporting its direct association with the presence of oxygen impurities. Additionally, both h-BN:O and undoped h-BN samples exhibit emission lines in the spectral range between 3.5 and 4.3 eV. The physical origins of these lines are to be determined.

Here, our focus will be on the nature of the 5.33 eV emission line. Given that h-BN possesses an indirect bandgap, <sup>17–23</sup> radiative recombination frequently requires phonon participation to conserve momentum. This inherent requirement explains the broad spectral linewidth observed for the 5.33 eV line. Below-bandgap emissions associated with impurities generally fall into two categories: band-to-impurity

transitions and donor–acceptor pair (DAP) transitions. To ascertain the nature of these specific emission lines, we investigated the temporal response of the 5.33 eV emission, with the results presented in Fig. 2(b). The decay of the 5.33 eV emission line is well-described by a single exponential function, yielding a decay lifetime ( $\tau$ ) of 0.51 ns. Since DAP transitions typically exhibit much longer lifetimes (on the order of  $\mu$ s to ms), the sub-ns decay lifetime observed here is a characteristic signature of a band-to-impurity transition. Based on this observed decay lifetime of 0.51 ns and the near absence of the 5.33 eV line in the undoped h-BN sample, we confidently assign the 5.33 eV emission line in the h-BN:O sample to the recombination between electrons bound to  $O_N$  donors and free holes in the valence band.

To resolve phonon-assisted peaks, higher-resolution PL spectra were taken at 10-80 K in the spectral range of 4.8-6.2 eV. Reducing the measurement temperature causes a slight blueshift in the position of the dominant peak near 5.33 eV, which is consistent with the expected temperature-dependent variation of the bandgap of semiconductors. Additionally, a weaker peak emerges on the higherenergy side of the spectrum as the temperature decreases. At 10 K, the PL spectrum clearly resolved two peaks at  $E_1 = 5.48\,\mathrm{eV}$  and  $E_2 = 5.33\,\mathrm{eV}$ . While the wavefunction of an electron bound to an oxygen donor is more localized at M-point in the k-space, it can extend to multiple valleys in k-space covering both M- and K-points because of the deep-level nature of O<sub>N</sub>.<sup>27</sup> Therefore, the direct band-to-impurity transition involving O<sub>N</sub> donors and the valence band in h-BN can occur without the participation of phonons. Based on this understanding and using the measured values of the room temperature energy bandgap of 6.02 eV<sup>28</sup> and activation energy of  $O_N$  donors of  $E_D = 0.56 \text{ eV}$ , the observed  $E_1 = 5.48 \text{ eV}$  emission line can confidently be assigned to the zero-phonon line (ZPL) of the band-to-impurity transition involving O<sub>N</sub> donors and the valence band.

Excitonic transitions in high-quality h-BN materials are typically assisted by phonons near the T-point in the first BZ to satisfy



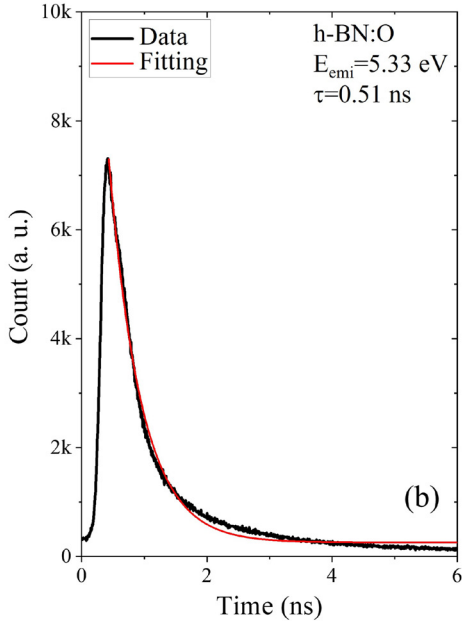


**FIG. 2.** (a) Low temperature (10 K) PL emission spectra of undoped h-BN (black curve) and h-BN:O (red curve) samples. (b) PL decay profile measured at 5.33 eV in a h-BN:O sample.

momentum conservation.  $^{21-23,47}$  Examining the two emission lines, a set of energy separations can be recognized,

$$\Delta E = E_1 - E_2 = (5.48 - 5.33) \,\text{eV} = 0.15 \,\text{eV}.$$

Figure 3(b) displays the phonon dispersion relations of h-BN along the main symmetry directions. While the electron wavefunction bound to an oxygen donor can extend to multiple valleys in k-space, encompassing both M- and K-points, the hole wavefunction remains highly localized at the K-point. Consequently, it is not surprising that the band-to-impurity transition involving  $O_N$  donors and the valence band is predominantly assisted by phonons at the K-point via a strong hole–phonon interaction. Indeed, the observed energy separation of  $\Delta E = 0.15 \, \mathrm{eV}$  corresponds well with the LO phonon mode at the K-point, as indicated by the green circle in Fig. 3(b).

More specifically, we can assign the main emission peak appearing at  $E_1=5.48\,\mathrm{eV}$  to the ZPL with the optical transition process described by a classical description of  $hv=E_g$ - $E_D$ , with  $E_g$  denoting the bandgap energy, and  $E_D$  the donor energy level, whereas the other peak is described by  $hv=E_g-E_D-E_p$ , with (-) sign expressing the emission process being assisted by emitting a phonon. Therefore, the other main peak at  $E_2=5.33\,\mathrm{eV}$  is the same transition associated with emission of an LO (K) phonon,  $E_2=E_1-\mathrm{LO}\left(\mathrm{K}\right)=\left(5.48-0.15\right)\mathrm{eV}=5.33\,\mathrm{eV}$ .

Based on the experimental results, we have constructed an energy diagram in Fig. 4 to detail the mechanism behind the observed emission lines at 5.33 and 5.48 eV. The 5.48 eV line is attributed to the recombination between free holes in the VBM at the K-point and electrons bound to O<sub>N</sub> donors, where the electron wavefunction is more localized around the M-point. The 5.33 eV emission line is the one phonon replica of the 5.48 eV line involving an LO (K) phonon of 0.15 eV. A significant difference exists between intrinsic exciton transitions and the band-to-impurity transitions in h-BN. For exciton transitions, phonon involvement is typically required to satisfy momentum conservation. However, for the band-to-impurity transition discussed here, the requirement for strict momentum conservation can be

relaxed. This is because the electron wavefunction bound to a deep  $O_{\rm N}$  donor ( $E_{\rm D}=0.56\,{\rm eV}$ ) extends to multiple symmetry points in k-space. This broad distribution of the donor-bound electron wavefunction in the k-space contrasts sharply with that of free electrons in the conduction band, which are highly localized at the M-point.

Despite this relaxation of momentum conservation for the ZPL, emission lines involving phonons can still exhibit higher or comparable intensity. We believe that this is the primary reason why most previously reported results show the 5.48 eV (ZPL) line to be weaker than the 5.33 eV emission line, which involves an LO (K) phonon. Indeed, as shown in Fig. 3, the 5.33 eV transition involving the LO (K) phonon exhibits a higher emission intensity than the ZPL at 5.48 eV. With the above understanding, several interesting comparisons can be made:

- (1) Band-to-impurity vs free exciton transitions in h-BN: In perfect h-BN, the electron wavefunction is localized at the M-point and the hole wavefunction at the K-point in k-space. The ZPL of free exciton transitions in perfect h-BN is thus forbidden or "dark." This explains why the exciton transitions observed in h-BN are invariably accompanied by strong exciton–phonon interaction, primarily involving T-point phonons. In contrast, for the band-to-impurity transitions investigated here, the wavefunctions of electrons bound to  $O_{\rm N}$  donors are spread in k-space. This delocalization of the wavefunction in the k-space allows the ZPL of the band-to-impurity transition to occur.
- (2) Band-to-impurity transitions in h-BN vs in AlN (and GaN): Band-to-impurity transitions in h-BN are distinctly different from those in other III-nitrides like GaN and AlN, all of which possess direct energy bandgaps. In h-BN, the wavefunction of an electron bound to an O<sub>N</sub> donor primarily reflects the characteristics of the conduction band at the M-point, while free hole wavefunctions are localized at the K-point. Conversely, in direct bandgap nitride semiconductors, band-to-impurity transitions involve only one extreme point in the BZ, typically the Γ-point. Consequently, the band-to-impurity transitions in

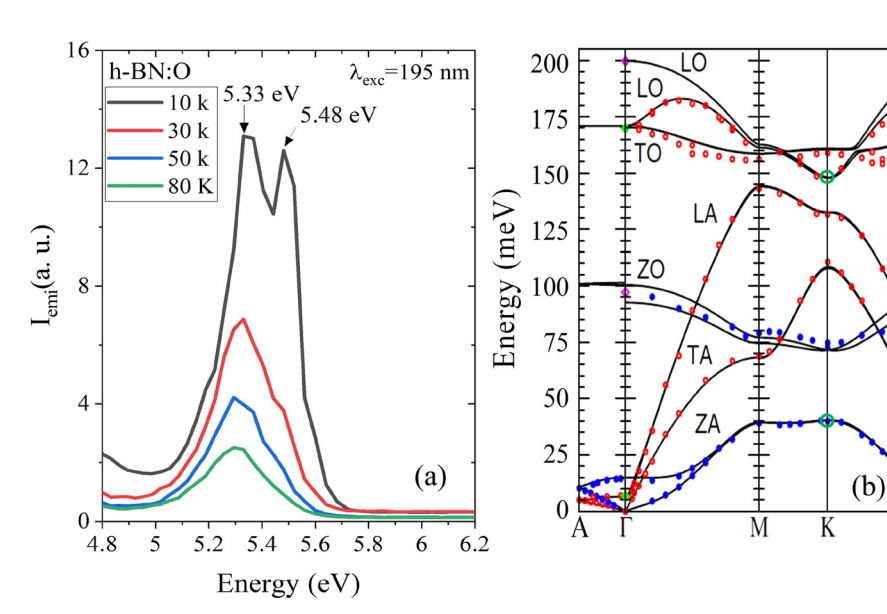
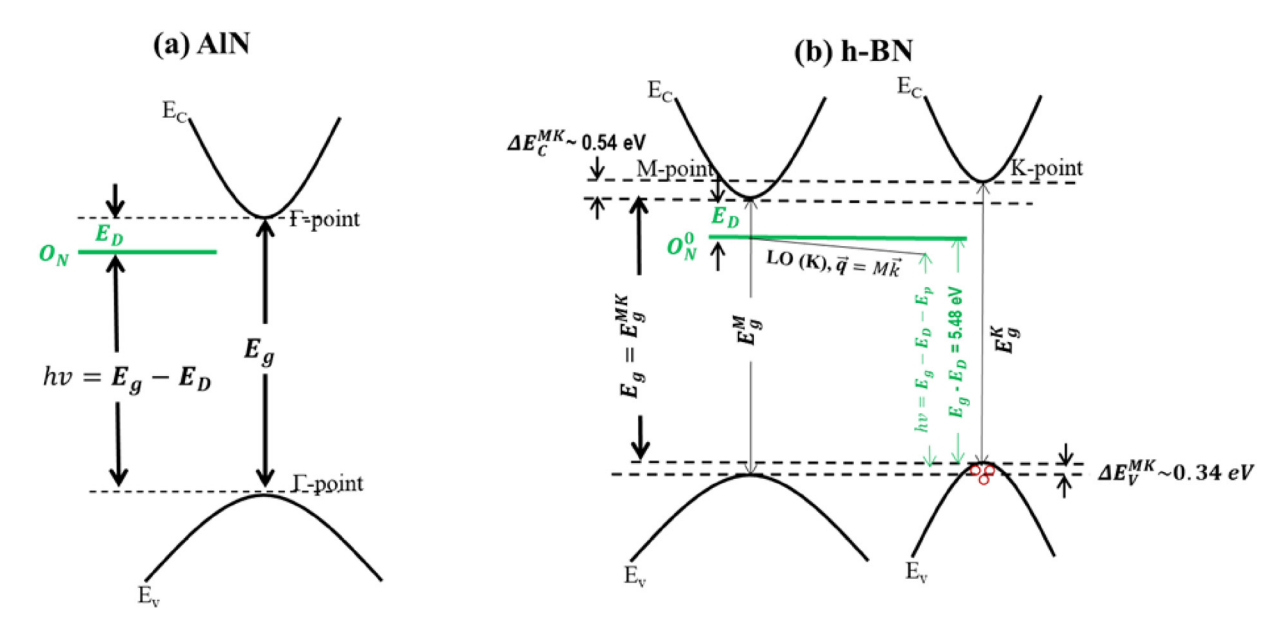


FIG. 3. (a) Low temperature (10 K-80 K) PL spectra of a h-BN:O sample measured from 4.8 to 6.2 eV. (b) The phonon dispersion relations of h-BN along the main symmetry directions. Reproduced with permission from Serrano et al., Phys. Rev. Lett. 98, 095503 (2007). Copyright 2007 American Physical Society.



**FIG. 4.** Energy diagrams of the band-to-impurity transitions in AlN and h-BN: (a) the band-to-impurity transitions in AlN occur without the need for phonon participation. (b) The band-to-impurity transitions involving electrons bound to oxygen donors and photoexcited free holes at the K-point in the valence band occur via a strong free-hole and K-point phonon interaction.

h-BN are accompanied by a much stronger free carrier-phonon interaction than those observed in other direct bandgap nitride semiconductors.

In summary, intentionally oxygen-doped h-BN epilayers have been produced using HVPE for the investigation of the band-to-impurity transitions involving oxygen donors. Our photoluminescence results conclusively resolved the physical origins of the commonly observed 5.33 and 5.48 eV emission lines in h-BN, which originate from the recombination between electrons bound to ON donors and free holes in the valence band, along its phonon replicas involving Kpoint phonons via free hole-phonon interaction. Our findings reveal several distinct features of band-to-impurity transitions in h-BN. First, although h-BN is an indirect bandgap semiconductor, the zerophonon line of the band-to-impurity transitions can occur with a sizeable probability. This is attributed to the deep-level nature of O<sub>N</sub> donors, which causes their bound electron wavefunctions to spread significantly in k-space, coupled with the small energy splitting between the M- and K-points in h-BN's conduction band. These results provide a more coherent understanding of the optical properties of impurity transitions in h-BN, which is crucial for advancing h-BN material and device technologies.

The information, data, or work presented herein was funded in part by the Advanced Research Projects Agency-Energy (ARPA-E) under the OPEN program, U.S. Department of Energy (Award No. DE-AR0001552), monitored by Dr. Olga Spahn and Dr. Eric Carlson. The views and opinions of authors expressed herein do not necessarily state or reflect those of the United States Government or any agency thereof. Jiang and Lin are grateful to the AT&T Foundation for the support of the Ed Whitacre and Linda Whitacre endowed chairs.

## AUTHOR DECLARATIONS Conflict of Interest

The authors have no conflicts to disclose.

#### **Author Contributions**

**Z.** Alemoush: Data curation (equal); Formal analysis (equal); Investigation (equal); Methodology (equal); Software (equal); Validation (equal); Visualization (equal). M. Almohammad: Data curation (equal); Formal analysis (equal); Investigation (equal); Software (equal); Validation (equal); Visualization (equal). J. Li: Data curation (equal); Formal analysis (equal); Investigation (equal); Methodology (equal); Software (equal); Supervision (equal); Validation (equal); Visualization (equal). J. Y. Lin: Conceptualization (equal); Funding acquisition (equal); Investigation (equal); Methodology (equal); Project administration (equal); Resources (equal); Supervision (equal); Validation (equal); Visualization (equal); Writing - original draft (equal); Writing - review & editing (equal). H. X. Jiang: Conceptualization (equal); Formal analysis (equal); Funding acquisition (equal); Investigation (equal); Methodology (equal); Project administration (equal); Resources (equal); Supervision (equal); Validation (equal); Visualization (equal); Writing original draft (equal); Writing - review & editing (equal).

#### **DATA AVAILABILITY**

The data that support the findings of this study are available within the article.

#### REFERENCES

<sup>1</sup>T. Sugino, K. Tanioka, S. Kawasaki, and J. Shirafuji, "Characterization and field emission of sulfur-doped boron nitride synthesized by plasma-assisted chemical vapor deposition," Jpn. J. Appl. Phys. **36**(Part 2), L463 (1997).

- <sup>2</sup>K. Watanabe, T. Taniguchi, and H. Kanda, "Direct-bandgap properties and evidence for ultraviolet lasing of hexagonal boron nitride single crystal," Nat. Mater. 3(6), 404 (2004).
- <sup>3</sup>Y. Kubota, K. Watanabe, O. Tsuda, and T. Taniguchi, "Deep ultraviolet light-emitting hexagonal boron nitride synthesized at atmospheric pressure," Science 317, 932 (2007).
- <sup>4</sup>R. Dahal, J. Li, S. Majety, B. N. Pantha, X. K. Cao, J. Y. Lin, and H. X. Jiang, "Epitaxially grown semiconducting hexagonal boron nitride as a deep ultraviolet photonic material," Appl. Phys. Lett. **98**, 211110 (2011).
- <sup>5</sup>A. Maity, T. C. Doan, J. Li, J. Y. Lin, and H. X. Jiang, "Realization of highly efficient hexagonal boron nitride neutron detectors," Appl. Phys. Lett. **109**, 072101 (2016).
- <sup>6</sup>A. Maity, S. J. Grenadier, J. Li, J. Y. Lin, and H. X. Jiang, "Toward achieving flexible and high sensitivity hexagonal boron nitride neutron detectors," Appl. Phys. Lett. 111, 033507 (2017).
- <sup>7</sup>A. Maity, S. J. Grenadier, J. Li, J. Y. Lin, and H. X. Jiang, "High efficiency hexagonal boron nitride neutron detectors with 1 cm<sup>2</sup> detection areas," Appl. Phys. Lett. 116, 142102 (2020).
- <sup>8</sup>A. Tingsuwatit, A. Maity, S. J. Grenadier, J. Li, J. Y. Lin, and H. X. Jiang, "Boron nitride neutron detector with the ability for detecting both thermal and fast neutron," Appl. Phys. Lett. **120**, 232103 (2022).
- <sup>9</sup>Z. Alemoush, A. Tingsuwatit, A. Maity, J. Li, J. Y. Lin, and H. X. Jiang, "Status of h-BN quasi-bulk crystals and high efficiency neutron detectors," J. Appl. Phys. 135, 175704 (2024).
- 10 J. Li, A. Tingsuwatit, Z. Alemoush, J. Y. Lin, and H. X. Jiang, "Ultrawide bandgap semiconductor h-BN for direct detection of fast neutrons," APL Mater. 13, 011101 (2025).
- <sup>11</sup>G. Somasundaram, N. K. Hossain, Z. Alemoush, A. Tingsuwatit, J. Li, J. Y. Lin, and H. X. Jiang, "Development of millimeter-thick hexagonal boron nitride wafers and fast neutron detectors," Appl. Phys. Lett. 126, 212104 (2025).
- <sup>12</sup>R. Bourrellier, S. Meuret, A. Tararan, O. Stephan, M. Kociak, L. H. G. Tizei, and A. Zobelli, "Bright UV single photon emission at point defects in h-BN," Nano Lett. 16, 4317 (2016).
- <sup>13</sup>A. K. Geim and I. V. Grigorieva, "Van der Waals heterostructures," Nature 499, 419 (2013).
- 14Y. Wu, Y. Xiao, Y. Zhao, and Z. Mi, "Van der Waals quantum dots on layered hexagonal boron nitride," Proc. Natl. Acad. Sci. 122, e2417859122 (2025).
- <sup>15</sup>Y. Gao, X. Lin, T. Smart, P. Ci, K. Watanabe, T. Taniguchi, R. Jeanloz, J. Ni, and J. Wu, "Band engineering of large-twist-angle graphene/h-BN moiré superlattices with pressure," Phys. Rev. Lett. 125, 226403 (2020).
- <sup>16</sup> Properties of Advanced Semiconductor Materials: GaN, AIN, InN, BN, SiC, SiGe, edited by M. E. Levinshtein, S. L. Rumyantsev, and M. S. Shur (John Wiley & Sons, 2001).
- <sup>17</sup>B. Arnaud, S. Lebègue, P. Rabiller, and M. Alouani, "Huge excitonic effects in layered hexagonal boron nitride," Phys. Rev. Lett. 96, 026402 (2006).
- <sup>18</sup>L. Wirtz, A. Marini, and A. Rubio, "Excitons in boron nitride nanotubes: Dimensionality effects," Phys. Rev. Lett. 96, 126104 (2006).
- <sup>19</sup>L. Wirtz, A. Marini, M. Gruning, C. Attaccalite, G. Kresse, and A. Rubio, "Huge excitonic effects in layered hexagonal boron nitride," Phys. Rev. Lett. 100, 189701 (2008).
- 20 J. Serrano, A. Bosak, R. Arenal, M. Krisch, K. Watanabe, T. Taniguchi, H. Kanda, A. Rubio, and L. Wirtz, "Vibrational properties of hexagonal boron nitride: Inelastic x-ray scattering and ab initio calculations," Phys. Rev. Lett. 98, 095503 (2007).
- <sup>21</sup>G. Cassabois, P. Valvin, and B. Gil, "Hexagonal boron nitride is an indirect bandgap semiconductor," Nat. Photonics 10, 262 (2016).
- 22L. Artús, M. Feneberg, C. Attaccalite, J. H. Edgar, J. Li, R. Goldhahn, and R. Cuscó, "Ellipsometry study of hexagonal boron nitride using synchrotron radiation: Transparency window in the far-UVC," Adv. Photonics Res. 2, 2000101 (2021).
- <sup>23</sup>T. Q. P. Vuong, G. Cassabois, P. Valvin, V. Jacques, A. Van Der Lee, A. Zobelli, K. Watanabe, T. Taniguchi, and B. Gil, "Phonon symmetries in hexagonal boron nitride probed by incoherent light emission," 2D Mater. 4, 011004 (2016).
- <sup>24</sup>Y. Hattori, T. Taniguchi, K. Watanabe, and K. Nagashio, "Anisotropic dielectric breakdown strength of single crystal hexagonal boron nitride," ACS Appl. Mater. Interfaces 8, 27877 (2016).

- 25Y. Hattori, T. Taniguchi, K. Watanabe, and K. Nagashio, "Comparison of device structures for the dielectric breakdown measurement of hexagonal boron nitride," Appl. Phys. Lett. 109, 253111 (2016).
- <sup>26</sup>C. Yuan, J. Li, L. Lindsay, D. Cherns, J. W. Pomeroy, S. Liu, J. H. Edgar, and M. Kuball, "Modulating the thermal conductivity in hexagonal boron nitride via controlled boron isotope concentration," Commun. Phys. 2, 43 (2019)
- <sup>27</sup>S. J. Grenadier, A. Maity, J. Li, J. Y. Lin, and H. X. Jiang, "Origin and roles of oxygen impurities in hexagonal boron nitride epilayers," Appl. Phys. Lett. 112, 162103 (2018).
- <sup>28</sup>N. K. Hossain, A. Tingsuwatit, Z. Alemoush, M. Almohammad, J. Li, J. Y. Lin, and H. X. Jiang, "Probing room temperature indirect and minimum direct band gaps of h-BN," Appl. Phys. Express 17, 091001 (2024).
- <sup>29</sup>L. Weston, D. Wickramaratne, M. Mackoit, A. Alkauskas, and C. G. Van de Walle, "Native point defects and impurities in hexagonal boron nitride," Phys. Rev. B 97, 214104 (2018).
- <sup>30</sup>F. Oba, A. Togo, I. Tanaka, K. Watanabe, and T. Taniguchi, "Doping of hexagonal boron nitride via intercalation: A theoretical prediction," Phys. Rev. B 81, 075125 (2010).
- <sup>31</sup>G. A. Slack, L. J. Schowalter, D. Morelli, and J. A. Freitas, "Some effects of oxygen impurities on AlN and GaN," J. Cryst. Growth 246, 287 (2002).
   <sup>32</sup>R. Y. Korotkov and B. W. Wessels, "Electrical properties of oxygen doped GaN
- <sup>32</sup>R. Y. Korotkov and B. W. Wessels, "Electrical properties of oxygen doped GaN grown by metalorganic vapor phase epitaxy," MRS Internet J. Nitride Semicond. Res. 5, 301 (2000).
- <sup>33</sup>Y. Zhang, J. Yang, F. Liang, Z. Liu, Y. Hou, B. Liu, F. Zheng, X. Liu, and D. Zhao, "Oxygen and point defect-related luminescence in AlN epitaxial layers grown by MOCVD," Opt. Lett. 50, 2498 (2025).
  <sup>34</sup>J. Li, K. B. Nam, M. L. Nakarmi, J. Y. Lin, H. X. Jiang, P. Carrier, and S.-H.
- <sup>34</sup>J. Li, K. B. Nam, M. L. Nakarmi, J. Y. Lin, H. X. Jiang, P. Carrier, and S.-H. Wei, "Band structure and fundamental optical transitions in wurtzite AlN," Appl. Phys. Lett. 83, 5163 (2003).
- <sup>35</sup>K. Era, F. Minami, and T. Kuzuba, "Fast luminescence from carbon-related defects of hexagonal boron nitride," J. Lumin. 24–25, 71 (1981).
- <sup>36</sup>M. R. Uddin, J. Li, J. Y. Lin, and H. X. Jiang, "Probing carbon impurities in hexagonal boron nitride epilayers," Appl. Phys. Lett. 110, 182107 (2017).
- 37T. Pelini, C. Elias, R. Page, L. Xue, S. Liu, J. Li, J. H. Edgar, A. Dreau, V. Jacques, P. Valvin, B. Gil, and G. Cassabois, "Shallow and deep levels in carbon-doped hexagonal boron nitride crystals," Phys. Rev. Mater. 3, 094001 (2019).
- 38M. Maciaszek, L. Razinkovas, and A. Alkauskas, "Thermodynamics of carbon point defects in hexagonal boron nitride," Phys. Rev. Mater. 6, 014005 (2022).
- 39M. Mackoit-Sinkevicien\_, M. Maciaszek, C. G. Van de Walle, and A. Alkauskas, "Carbon dimer defect as a source of the 4.1 eV luminescence in hexagonal boron nitride," Appl. Phys. Lett. 115, 212101 (2019).
- <sup>40</sup>C. A. Taylor, S. W. Brown, V. Subramaniam, S. Kidner, S. C. Rand, and R. Clarke, "Observation of near-band-gap luminescence from boron nitride films," Appl. Phys. Lett. 65, 1251 (1994).
- <sup>41</sup>X. Z. Du, J. Li, J. Y. Lin, and H. X. Jiang, "The origins of near band-edge transitions in hexagonal boron nitride epilayers," Appl. Phys. Lett. 108, 052106 (2016)
- <sup>42</sup>G. Cassabois, P. Valvin, and B. Gil, "Intervalley scattering in hexagonal boron nitride," Phys. Rev. B 93, 035207 (2016).
- <sup>43</sup>L. Museur and A. Kanaev, "Near band-gap photoluminescence properties of hexagonal boron nitride," Appl. Phys. Lett. 103, 103520 (2008).
- <sup>44</sup>R. Bourrellier, M. Amato, L. Henrique, G. Tizei, C. Giorgetti, A. Gloter, M. I. Heggi, K. March, O. Stephan, L. Reining, M. Kociak, and A. Zobelli, "Nanometric resolved luminescence in h-BN flakes: Excitons and stacking order," ACS Photonics 1, 857 (2014).
- <sup>45</sup>K. Watanabe, T. Taniguchi, T. Kuroda, and H. Kanda, "Effects of deformation on band-edge luminescence of hexagonal boron nitride single crystals," Appl. Phys. Lett. 89, 141902 (2006).
- <sup>46</sup>Q. W. Wang, J. Li, J. Y. Lin, and H. X. Jiang, "Probing the surface oxidation process in hexagonal boron nitride epilayers," AIP Adv. 10, 025213 (2020).
- <sup>47</sup>J. Li, J. Y. Lin, and H. X. Jiang, "Fundamental optical transitions in hexagonal boron nitride epilayers," APL Mater. 12, 111115 (2024).